doi:10.1093/brain/awab018 BRAIN 2021: 144; 1214–1229 | 1214

BRAIN
A JOURNAL OF NEUROLOGY

A serum microRNA sequence reveals fragile X protein pathology in amyotrophic lateral sclerosis

Axel Freischmidt,[1,2] Anand Goswami,[3] Katharina Limm,[4] Vitaly L. Zimyanin,[5,6] Maria Demestre,[7] Hannes Glaß,[8] Karlheinz Holzmann,[9] Anika M. Helferich,[1] Sarah J. Brockmann,[1] Priyanka Tripathi,[3] Alfred Yamoah,[3] Ina Poser,[10] Peter J. Oefner,[4] Tobias M. Böckers,[2,7] Eleonora Aronica,[11] Albert C. Ludolph,[1,2] Peter M. Andersen,[12] Andreas Hermann,[5,8,13,14] Joachim Weis,[3] Jörg Reinders,[4] Karin M. Danzer[1] and Jochen H. Weishaupt[1,15]

Knowledge about converging disease mechanisms in the heterogeneous syndrome amyotrophic lateral sclerosis (ALS) is rare, but may lead to therapies effective in most ALS cases. Previously, we identified serum microRNAs downregulated in familial ALS, the majority of sporadic ALS patients, but also in presymptomatic mutation carriers. A 5-nucleotide sequence motif (GDCGG; D = G, A or U) was strongly enriched in these ALS-related microRNAs. We hypothesized that deregulation of protein(s) binding predominantly to this consensus motif was responsible for the ALS-linked microRNA fingerprint. Using microRNA pull-down assays combined with mass spectrometry followed by extensive biochemical validation, all members of the fragile X protein family, FMR1, FXR1 and FXR2, were identified to directly and predominantly interact with GDCGG microRNAs through their structurally disordered RGG/RG domains. Preferential association of this protein family with ALS-related microRNAs was confirmed by *in vitro* binding studies on a transcriptome-wide scale. Immunohistochemistry of lumbar spinal cord revealed aberrant expression level and aggregation of FXR1 and FXR2 in *C9orf72*- and *FUS*-linked familial ALS, but also patients with sporadic ALS. Further analysis of ALS autopsies and induced pluripotent stem cell-derived motor neurons with *FUS* mutations showed co-aggregation of FXR1 with FUS. Hence, our translational approach was able to take advantage of blood microRNAs to reveal CNS pathology, and suggests an involvement of the fragile X-related proteins in familial and sporadic ALS already at a presymptomatic stage. The findings may uncover disease mechanisms relevant to many patients with ALS. They furthermore underscore the systemic, extra-CNS aspect of ALS.

1 Department of Neurology, Ulm University, Ulm, Germany
2 German Center For Neurodegenerative Diseases (DZNE) Ulm, Ulm, Germany
3 Institute of Neuropathology, RWTH Aachen University Hospital, Aachen, Germany
4 Institute of Functional Genomics, University of Regensburg, Regensburg, Germany
5 Department of Neurology, Technical University Dresden, Dresden, Germany
6 Department of Biology, University of Virginia, Charlottesville, VA, USA
7 Institute for Anatomy and Cell Biology, Ulm University, Ulm, Germany
8 Translational Neurodegeneration Section "Albrecht-Kossel", Department of Neurology, University Medical Center Rostock, University of Rostock, Rostock, Germany
9 Core Unit Genomics, Ulm University, Ulm, Germany
10 Max Planck Institute of Molecular Cell Biology and Genetics, Dresden, Germany
11 Amsterdam UMC, University of Amsterdam, Department of (Neuro)Pathology, Amsterdam Neuroscience, Amsterdam, The Netherlands

Received June 24, 2019. Revised October 19, 2020. Accepted November 11, 2020. Advance access publication April 19, 2021

12 Department of Clinical Science, Neurosciences, Umeå University, Umeå, Sweden
13 Center for Transdisciplinary Neurosciences Rostock (CTNR), University Medical Center Rostock, University of Rostock, Rostock, Germany
14 German Center for Neurodegenerative Diseases (DZNE) Rostock/Greifswald, Rostock, Germany
15 Division for Neurodegenerative Diseases, Neurology Department, University Medicine Mannheim, Heidelberg University, Mannheim, Germany

Correspondence to: Univ.-Prof. Dr. med. Jochen Weishaupt
Division for Neurodegenerative Diseases, Neurology Department, University Medicine Mannheim, Heidelberg University, Theodor-Kutzer-Ufer 1-3, 68167 Mannheim, Germany
E-mail: jochen.weishaupt@medma.uni-heidelberg.de

Keywords: amyotrophic lateral sclerosis; miRNA; FMR1/FMRP; FXR1; FXR2

Abbreviations: α-MN = alpha motor neuron; EMSA = electrophoretic mobility shift assay; f/sALS = familial/sporadic amyotrophic lateral sclerosis; FXP = fragile X protein; iPSC = induced pluripotent stem cell

Introduction

Mutations in more than 30 genes lead to the clinical phenotype of familial amyotrophic lateral sclerosis (fALS), which is caused primarily by the degeneration of motor neurons in the motor cortex, brainstem and spinal cord. The inheritance mode of fALS is usually autosomal-dominant. However, more than 90% of ALS cases develop the disease sporadically (sALS), without an apparent family history. Histopathological hallmarks of ALS are ubiquitinated proteinaceous cytoplasmic inclusions in affected tissues. In the vast majority of sALS and fALS patients, these inclusions contain the protein TDP-43 (encoded by *TARDBP*). Exceptions are *SOD1*- and *FUS*-linked ALS, where aggregates largely lack TDP-43, but contain SOD1 or FUS protein, respectively.[1-3]

Genetic and functional evidence points towards four main cell biological topics that are related to ALS, namely protein homeostasis, RNA metabolism, cytoskeletal dynamics and possibly DNA damage/repair.[3,4] It is tempting to hypothesize that different causative factors converge on a few pathways ultimately resulting in the relatively specific death of the motor neuronal subpopulation of CNS neurons. This is also supported by experimental protein-protein interaction studies[5] as well as *in silico* network analyses of ALS-related proteins,[6] which revealed common binding partners and mutual interactions of different proteins genetically associated with ALS. Therefore, considerable evidence supports the existence of common downstream events, at least for some ALS-related proteins. Nevertheless, knowledge about converging molecular disease mechanisms in the heterogeneous syndrome ALS is rare.

In previous studies, we identified a subset of microRNAs (miRNAs) downregulated in serum that was independent of the underlying disease gene, specifically in patients with mutations in *SOD1*, *C9orf72* and *FUS*.[7,8] Although it remained unclear whether extracellular miRNAs causally contribute to diseases there is a consensus that many disease conditions are at least reflected in changes of extracellular miRNA profiles.[9] The ALS-linked miRNA patterns were partially already evident in presymptomatic carriers of highly penetrant ALS mutations (*SOD1*, *C9orf72* and *PFN1*), indicating that they mirror early pathogenic events and excluding secondary effects such as immobility or medication of ALS patients as possible causes.[7] Additionally, downregulation of the ALS-related miRNAs was also evident in ∼60% of sporadic patients suggesting alteration of similar pathogenic pathways as in familial cases in the majority of sALS cases.[8]

Most strikingly, among the 22 miRNAs differentially regulated in ALS and presymptomatic ALS mutation carriers (herein after referred to as the 'ALS-related miRNA profile'; Supplementary Table 1), miRNAs containing a 5-nucleotide sequence motif (GDCGG; D = G, A or U)[7] were highly enriched when compared to the background of all miRNAs. Therefore, in this work we test the hypothesis that one or several RNA-binding protein(s) that are deregulated in regard to their function, expression and/or localization in sALS and fALS patients bind to the GDCGG motif. We present evidence that these miRNAs directly interact with the three members of the fragile X protein (FXP) family (FMR1, FXR1 and FXR2) *in vitro*, and show neuropathological alterations of FXR1 and FXR2 in *FUS*- and *C9orf72*-linked fALS and in sALS.

Materials and methods

Patient cohorts and ethics statement

ALS patients participating in this study were diagnosed for definite ALS according to the revised El Escorial criteria.[10] Genotyping of ALS patients was performed as previously described[11] and patients were considered sporadic cases due to a negative family history of the disease and absence of mutations in *SOD1* and *C9orf72*, the most frequent causes of fALS.[2,3]

This study was approved by the national ethical review boards according to the declaration of Helsinki (WMA, 1964) and informed written consent was provided by all participating individuals.

Gene ontology analyses

Gene ontology analyses were performed using the DAVID Functional Annotation Tool (Version 6.8; https://david.ncifcrf.gov/).[12,13]

Expression and purification of recombinant proteins

Detailed information about the proteins expressed is listed in Supplementary Table 2. Experimental procedures for the purification of recombinant proteins are described in the Supplementary material.

Electrophoretic mobility shift assay

For electrophoretic mobility shift assays (EMSAs), 200 pmol of a synthetic miRNA (biomers) and 10–50 pmol of a recombinant protein in elution buffer were mixed in miRNA buffer in a total volume of 20 µl. To ensure equal salt concentrations and comparability of all EMSAs, the volume of the recombinant protein in elution buffer was kept constant (5 µl) in all assays. After an incubation on ice for 30 min, 5 µl of loading dye [50% glycerol, 10% Novex Hi-Density TBE sample buffer (5×) (Thermo Fisher Scientific #LC6678)] was added and the samples loaded onto 3% agarose gels prepared in 0.5× TBE (44.5 mM Tris, 44.5 mM boric acid, 1 mM EDTA, pH 8.3) containing 0.2 µg/ml ethidium bromide. Electrophoresis was carried out at 65 V for 75 min and a UV transilluminator was used to visualize the bands.

Protein/miRNA co-purification experiments

The protein of interest coupled to Ni-NTA Agarose (Qiagen #30210) was incubated with an equimolar mix of three to five synthetic miRNAs. After washing, co-purifying miRNAs were quantified using quantitative reverse transcription PCR (qRT-PCR). The experiment is described in detail in the Supplementary material. MiRNA-specific forward primers used are listed in Supplementary Table 3.

In silico prediction of RNA-binding amino acids

To predict stretches of amino acids in the disordered C-termini of FXR1 and FXR2 that putatively participate in RNA-binding, we used the RNABindRPlus software (http://ailab1.ist.psu.edu/RNABindRPlus/).[14]

Drawing of schematic diagrams of protein sequences

For the schematic presentation of protein sequences we used the 'Illustrator of Biological Sequences' (IBS; Version 1.0.1; http://ibs.biocuckoo.org/).[15]

Microarray analyses of miRNAs co-purifying with the RGG/RG domains of FXR1/FXR2/FMR1

Low molecular weight RNA isolated from HEK293 cells was incubated with the recombinant RGG/RG2-domains of FXR1, FXR2 or FMR1, respectively. After recovery of the respective domains, co-purifying RNAs were compared to the input RNA using Affymetrix miRNA 3.0 arrays. A detailed description of the procedure including statistical analysis can be found in the Supplementary material.

Hierarchical cluster analyses

Hierarchical cluster analyses (average linkage) of miRNAs binding to the RGG/RG2-domains of FMR1, FXR1 and FXR2 were performed using the Genesis software package (http://genome.tugraz.at/).[16]

RNA immunoprecipitation

A detailed description of RNA-immunoprecipitation of myc-tagged and endogenous FXR1 from lysates of HEK293 cells is provided in the Supplementary material. Co-precipitating endogenous miRNAs were quantified by qRT-PCR using miScript Primer Assays (Qiagen; Supplementary Table 4).

Induced pluripotent stem cell-derived motor neurons

The generation of isogenic motor neurons expressing endogenously GFP-tagged FUS^{wt} or FUS^{P525L} is described elsewhere.[17] After differentiation, the cells were matured for ~2–3.5 weeks as described previously.[17,18] Stress granules were induced by addition of 0.2 mM sodium arsenite to the culture medium for 1 h.

The motor neurons carrying a $FUS^{D502Tfs27}$ mutation were described and characterized previously.[19] Induced pluripotent stem cells (iPSCs) were generated as described.[19,20] Differentiation of the iPSC colonies is described in the Supplementary material.

MiRNA fluorescence *in situ* hybridization

Simultaneous visualization of FXR1 and miR-92a-3p or miR-3665 in iPSC-derived motor neurons was performed with the ViewRNA™ Cell Plus Assay Kit (Thermo Fisher Scientific #88-19000-99) and ViewRNA™ Cell Plus miRNA Assays (Thermo Fisher Scientific #VM1-10463-VCP and #VM1–34581-VCP) according to the manufacturer's instructions.

Antibodies

Supplementary Table 5 lists all primary and secondary antibodies used for immunofluorescence staining and western blotting including manufacturer, catalogue number and working concentration used.

Additional protocols

Further details of the following experimental protocols can be found in the Supplementary material: cell lines, plasmids, siRNAs and transfection; miRNA-pull-down procedures using synthetic, 5′-biotinylated miRNAs in lysates of HEK293 cells; identification of GDCGG-binding proteins using label-free quantitative LC-MS/MS; isolation of fractions enriched in FXR1 and FXR2 from HEK293 cells; immunocytochemistry and microscopy (staining and imaging of cells in culture); quantification of miRNAs in iPSC-derived motor neurons and HAP1 cells using qRT-PCR; immunohistochemistry using diaminobenzidine (DAB) for human post-mortem spinal cord samples; glutathione-S-transferase (GST) pull-down assays; and immunofluorescence staining of post-mortem spinal cord sections.

Statistical analysis

Unpaired, two-tailed student's *t*-tests or Fisher's exact test were performed to analyse experiments. When appropriate, *P*-values were adjusted for multiple testing using false discovery rate (FDR) correction.[21] Statistical tests used are specified in the respective sections of the 'Materials and methods', 'Results' and/or in the figure legends. *P*-values/FDRs $\leqslant 0.05$ were considered statistically significant.

Data availability

All data associated with this study are present in the paper or Supplementary material. Microarray raw data can be accessed at Gene Expression Omnibus (http://www.ncbi.nlm.nih.gov/geo/). GSE number is GSE101067.

Results

Identification of proteins binding to GDCGG-motif-containing miRNAs

We have previously identified serum miRNAs downregulated in fALS and presymptomatic ALS mutation carriers. Among them, miRNAs containing a 5-nucleotide consensus sequence (GDCGG; D = G, A or U) were highly enriched when compared to the background of all miRNAs.[7] Consequently, to screen for proteins binding to GDCGG motif-containing miRNAs, we performed pull-down assays of biotinylated miRNAs using streptavidin beads, followed by mass spectrometric identification of co-precipitating proteins. Because of the high RNase-activity in serum and plasma that degrades exogenously added RNA within seconds,[22] and the very low abundance of most proteins in serum/plasma,[23] pull-downs were performed from HEK293 cell lysates. The most downregulated miRNAs in ALS[7] comprising one or two copies of the consensus motif served as baits, namely miR-4745-5p (GACGG) and miR-638 (two times GGCGG). As control baits, miR-638 with a mild (miR-638mut1) or a severe (miR-638mut2) mutation of the consensus motif were used. The *Caenorhabditis elegans* miRNA Cel-miR-39-3p without the consensus motif served as an additional negative control (Fig. 1A). All five miRNAs led to the precipitation of sufficient amounts of protein for reliable mass spectrometric analyses (Fig. 1B).

We identified and quantified 775 proteins in all pull-down samples ($n = 3$–4 for each miRNA; Supplementary Table 6) and a gene ontology analysis (molecular function) revealed a highly significant enrichment of poly(A) RNA-binding and RNA-binding proteins (corrected *P*-value = 0 and 1.57×10^{-115}, respectively; Supplementary Table 7). To select proteins specifically interacting with GDCGG miRNAs, we compared the abundance of proteins co-precipitating with miR-638wt versus miR-638mut1, miR-638wt versus miR-638mut2 as well as miR-4745-5p versus Cel-miR-39-3p. Only proteins that were at least 2-fold more abundant after pull-down with the miRNA that contains the motif compared to the respective control miRNA (corrected *P*-value $\leqslant 0.05$) were considered further. The 28 proteins fulfilling these criteria simultaneously in all three comparisons performed are listed in Fig. 1C and Supplementary Table 6.

The top two candidate proteins identified to bind to GDCGG-containing miRNAs were the fragile X-related proteins FXR1 and FXR2 (Fig. 1C and D), which were also the only two proteins from our earlier list of candidates implicated in miRNA pathways before. Both proteins are highly homologous to the third member of this family, FMR1.

Additionally, Fig. 1E shows the pull-down result for MRPS26, a mitochondrial ribosomal protein. MRPS26 represents the highest ranked protein candidate that missed our stringent selection criteria (Supplementary Table 6).

FXR1 directly and predominantly interacts with GDCGG miRNAs via its RGG domain

To validate the interaction of GDCGG-containing miRNAs with FXR1/FXR2, and to determine if the observed interactions are direct or rather mediated by adaptor proteins, we used EMSAs with recombinant FXR proteins and synthetic miRNAs.

We expressed and purified FXR1 as N-terminal (FXR1-N) and C-terminal (FXR1-C) fragments from *Escherichia coli*, as full-length FXR1 protein was not stable in solution. The two RNA-binding K-homology (KH) domains are located in the N-terminus, while the RNA-binding RGG-box is located C-terminally (Fig. 2A and D). Regarding FXR2, only the N-terminus (FXR2-N), comprising the two KH domains, was expressed and could be purified (Fig. 2B and D). The C-terminus harbouring two RNA-binding RG boxes was thus not accessible for EMSA. Additionally, we expressed and purified two full-length control proteins, GST and MRPS26, from *E. coli* (Fig. 2C and D). MRPS26 was the highest ranked protein that missed our stringent selection criteria, and was included at this stage as a control to validate these criteria. The recombinant proteins were fused to a

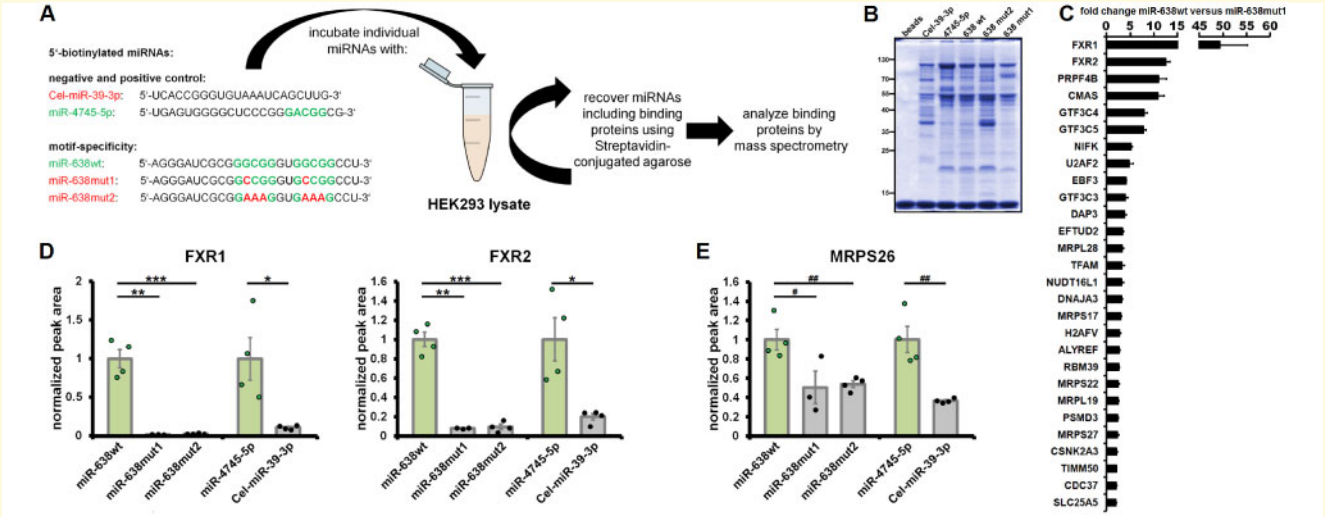

Figure 1 Discovery experiment identifying proteins closely associated with miRNAs comprising the GDCGG motif. (**A**) Workflow of miRNA pull-down experiments in lysates of HEK293 cells and sequences of 5′-biotinylated miRNAs used. (**B**) Representative SDS-PAGE of a typical miRNA pull-down experiment followed by staining with Coomassie brilliant blue. (**C**) List of the 28 candidate proteins (official gene symbols) putatively associated with GDCGG miRNAs (see main text for statistical details). The graph shows the fold change calculated from the most stringent comparison [miR-638wt versus miR-638mut1; $n = 3$–4; bars indicate mean ± standard error of the mean (SEM)]. (**D** and **E**) Results of the top two candidate proteins FXR1 and FXR2 (**D**), as well as of the highest ranked protein that missed our stringent selection criteria, MRPS26 (**E**), in all three statistical comparisons performed (miR-638wt versus miR-638mut1, miR-638wt versus miR-638mut2 and miR-4745-5p versus Cel-miR-39-3p; $n = 3$–4; bars indicate mean ± SEM. Corrected *P*-values: $^{*}P \leqslant 0.05$, $^{**}P \leqslant 0.01$, $^{***}P \leqslant 0.001$; uncorrected *P*-values: $^{\#}P \leqslant 0.05$, $^{\#\#}P \leqslant 0.01$.

C-terminal His_6-tag as well as to N-terminal GST- or T7-tags, respectively (Fig. 2A–C).

The results from EMSAs revealed a predominant interaction of FXR1-C, but not FXR1-N or FXR2-N, with GDCGG-containing miRNAs (Fig. 2E). The negative controls GST and MRPS26, fused to the same tags as the FXR proteins, did not show interaction with any of the miRNAs and further confirmed the specificity of FXR1-C/miRNA binding (Fig. 2E). EMSAs with additional miRNAs with and without the GDCGG motif, or with a single-nucleotide variation of the motif consistently revealed a stronger affinity of FXR1-C for miRNAs containing the intact motif (Fig. 2F and G).

As another line of evidence, we used Ni-NTA-based co-purification to prove preferential competitive binding of FXR1 to GDCGG-containing miRNAs. To that end, FXR1-C or full-length FXR1 protein was coupled to Ni-NTA beads and incubated with an equimolar mix of synthetic miRNAs with and without the motif. After washing, the miRNAs co-purifying with the beads were quantified by qRT-PCR. Both recombinant FXR1-C (Fig. 2H) as well as full-length FXR1 (Fig. 2I) showed a significantly higher affinity for GDCGG miRNAs when compared to miRNAs lacking the consensus motif. Taken together, several different technical approaches confirmed direct and predominant binding of the disordered C-terminus of FXR1 to the ALS-related GDCGG-containing miRNAs.

Next, we aimed to identify the specific domain in the C-terminus of FXR1 that mediates binding to GDCGG miRNAs. First, we tested if the shorter C-terminus of the known FXR1 splice isoform b (Supplementary Fig. 1A) is still capable of binding to GDCGG miRNAs and found similar RNA-binding properties as for isoform a (Supplementary Fig. 1E and F). *In silico* analysis of the C-terminus of FXR1 isoform b revealed three different amino acid stretches, including the RGG-domain of FXR1, predicted to bind to RNA (Supplementary Fig. 1B). Analyses of recombinant C-terminal fragments of FXR1 (Supplementary Fig. 1C and D) by EMSA revealed that the RGG-domain of FXR1, but not the other two domains predicted to bind RNA, binds directly and predominantly with high affinity to miRNAs comprising the GDCGG motif (Supplementary Fig. 1E and F).

FXR2 and FMR1 also directly and predominantly bind via their RGG/RG domains to GDCGG miRNAs

Next, we aimed to determine whether the two close homologues of FXR1, namely FXR2 and FMR1, were also predominantly interacting with the GDCGG miRNAs. For FXR2, the second top candidate protein of our initial discovery experiment (Fig. 1C, D and Supplementary Table 6), we applied a similar strategy as for FXR1. By *in silico* prediction of RNA-binding amino acids in the C-terminus of FXR2 and using EMSAs with recombinant C-terminal fragments and different miRNAs for validation, we found direct

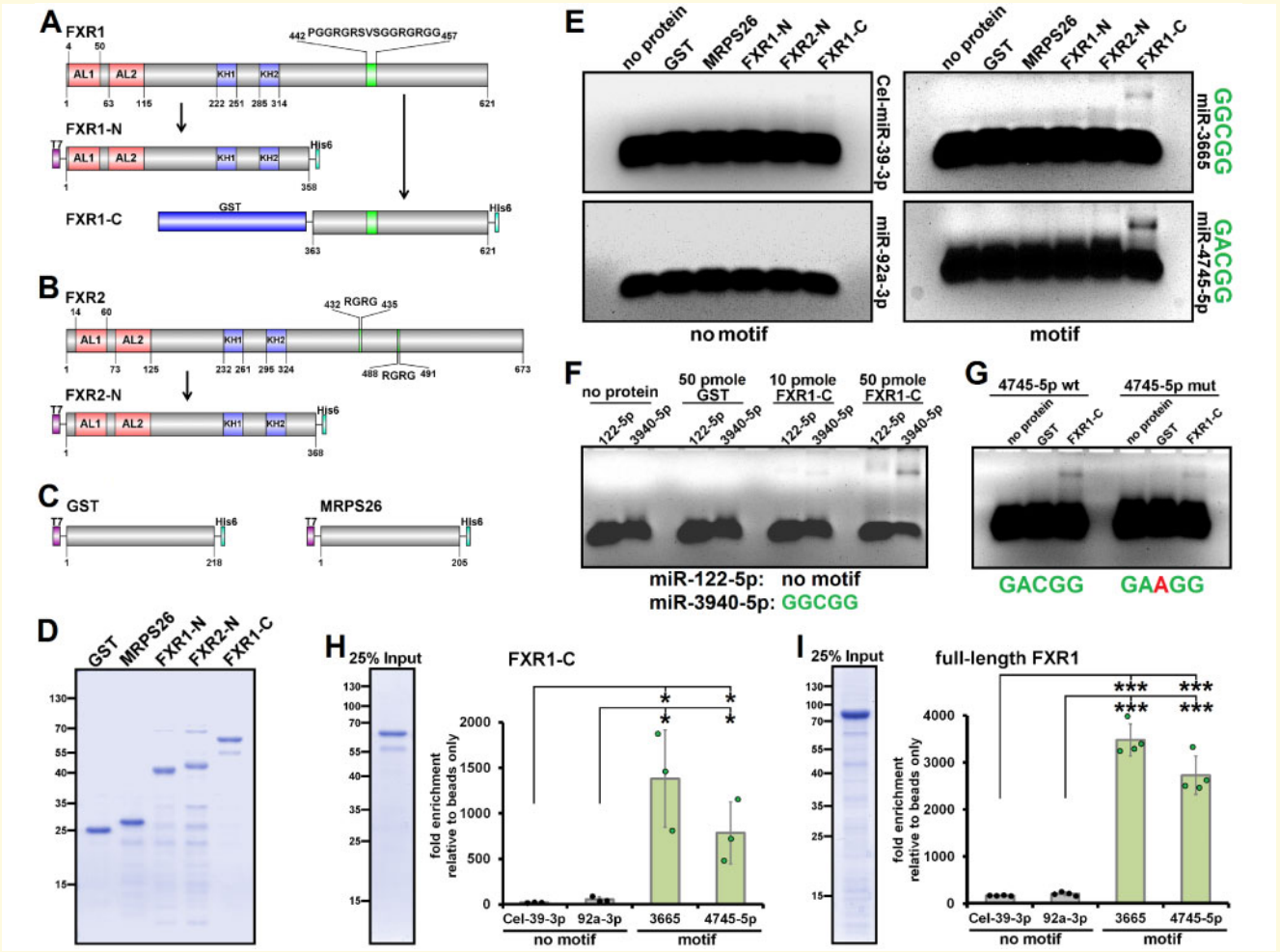

Figure 2 GDCGG miRNAs directly and predominantly interact with the C-terminus of FXR1. (**A** and **B**) Schematic presentation of full-length FXR1 (isoform a; **A**) and full-length FXR2 (**B**), as well as of the protein constructs purified from *E. coli* including the tags used for expression and purification. The RGG domain of FXR1 and the two RG boxes of FXR2 are indicated in green (AL = Agenet-like domain; KH = K homology domain; domains according to UniProt). (**C**) Schematic drawing of the control proteins used (GST and MRPS26). (**D**) SDS-PAGE stained with Coomassie brilliant blue shows the recombinant proteins purified from *E. coli* used for EMSAs in **E**–**G**. (**E**) EMSAs using 10 pmol of the recombinant proteins indicated and miRNAs with and without the GDCGG motif. (**F** and **G**) EMSAs directly comparing the affinity of FXR1-C for miRNAs with and without the GDCGG-motif (**F**) as well as for the same GDCGG miRNA upon mutation of a single nucleotide of the motif (**G**; 10 pmol of FXR1-C were used). (**H** and **I**) Protein/miRNA co-purification experiments quantifying miRNAs by qRT-PCR that co-purify with recombinant FXR1-C (**H**) and full-length FXR1 (**I**) coupled to Ni-NTA beads after incubation with equimolar mixtures of the miRNAs indicated. SDS-PAGEs stained with Coomassie brilliant blue of the recombinant proteins used for the assays are shown (n = 3–4; bars indicate mean ± SD; $^{*}P \leqslant 0.05$, $^{***}P \leqslant 0.001$ in an unpaired, two-tailed Student's t-test).

and predominant binding of the second RG domain (RG2 domain) of FXR2 to the ALS-related GDCGG miRNAs (Supplementary Fig. 2). Furthermore, using our Ni-NTA-based co-purification approach described above, we show that also eukaryotically-expressed full-length FXR1 and FXR2 preferentially interact with GDCGG miRNAs (Supplementary Fig. 3).

Reanalysis of our initial discovery experiment (Fig. 1) revealed that FMR1 was only excluded from further analyses because of the lack of statistical significance in one of the three comparisons included in our stringent selection criteria (preferential binding to miR-4745-5p compared to Cel-miR-39-3p). Nevertheless, a strong trend here (corrected P-value = 0.07) was also evident (Fig. 3A). An alignment of the RGG/RG2-domains of FXR1 and FXR2, respectively, with the RGG-domain of FMR1 revealed a high homology (Fig. 3B). Consequently, we compared binding of the RGG/RG2 domains of FXR1, FXR2 and FMR1 (Fig. 3C and D) to synthetic miRNAs with and without the GDCGG motif in EMSAs. All three protein fragments preferentially bound to GDCGG miRNAs (Fig. 3E and F). Furthermore, an miRNA pull-down using biotinylated miRNAs in lysates of HEK293 cells specifically precipitated all three FXPs with an miRNA that included the GDCGG motif (Fig. 3G).

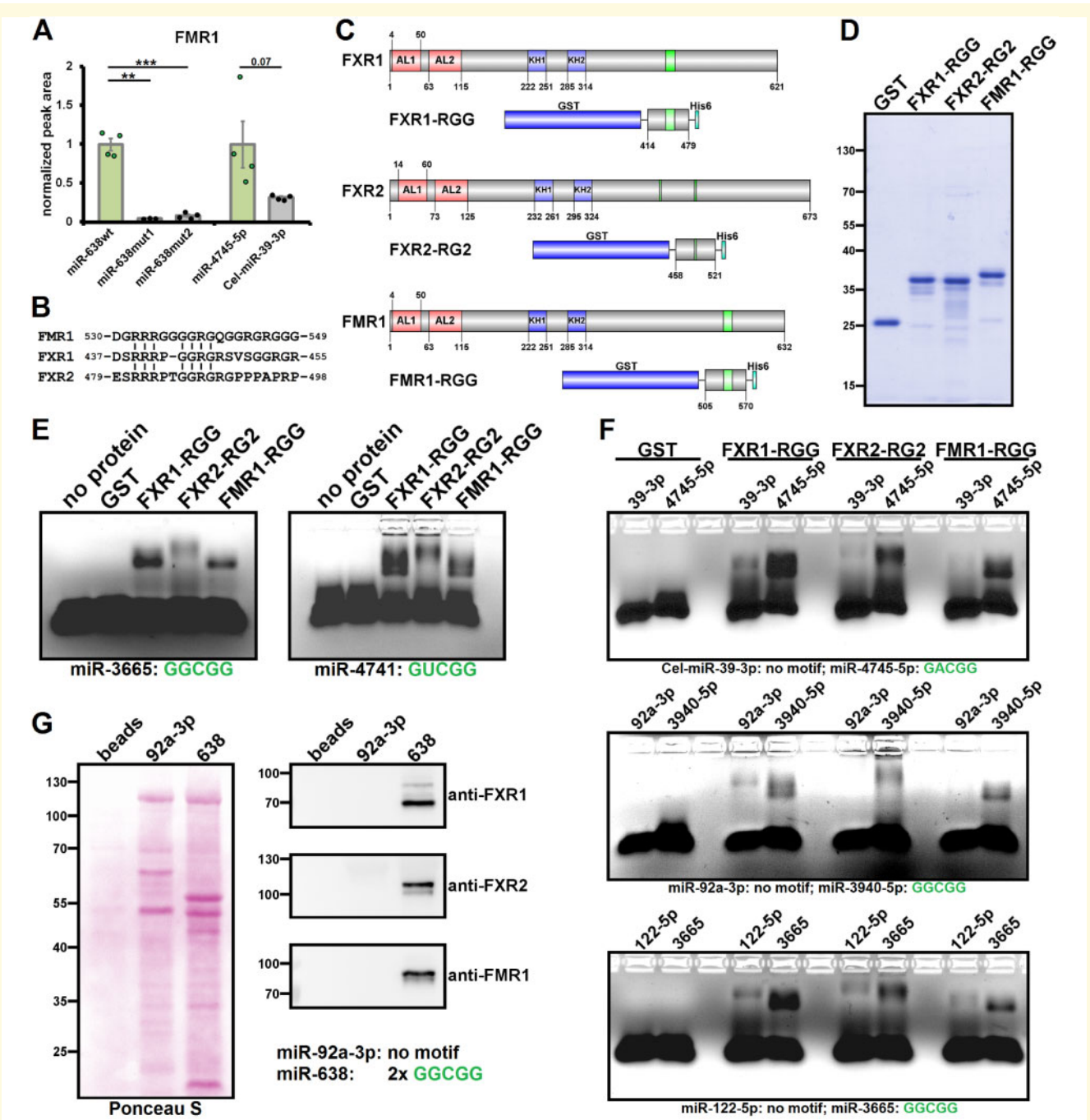

Figure 3 All three members of the FXP family directly and predominantly interact with ALS-related GDCGG-miRNAs. (**A**) Results of FMR1 in our initial discovery experiment (Fig. 1; n = 3–4; bars indicate mean ± SEM; corrected P-values: $^{**}P \leqslant 0.01$, $^{***}P \leqslant 0.001$). (**B**) Alignment of the RGG/RG2 domains of FXR1 and FXR2 with the RGG domain of FMR1. (**C**) Schematic presentation of full-length FXR1 (isoform a), FXR2 and FMR1 (isoform ISO1) as well as of the fusion constructs of the respective RGG/RG2 domains purified from *E. coli* (AL = Agenet-like domain; KH = K homology domain; RGG and RG domains are indicated in green; domains according to UniProt). (**D**) SDS-PAGE stained with Coomassie brilliant blue of the fusion proteins purified from *E.coli* and used for EMSAs. GST was fused to a N-terminal T7- and a C-terminal His_6-tag. (**E** and **F**) EMSAs of the RGG/RG2-domains of FXR1, FXR2 and FMR1 with GDCGG miRNAs (**E**) and direct comparison of the affinity of the respective RGG/RG2-domains for miRNAs with and without the motif (**F**). In all EMSAs shown, 50 pmol of protein was used. (**G**) Results of an miRNA pull-down assay in lysates of HEK293 cells using 5′-biotinylated miRNAs with and without the motif followed by western blot analyses. Ponceau S staining of the blot (*left*) and antibody detection of the FXP family members (*right*) are shown.

The RGG domain of FMR1 has been repeatedly shown to interact with RNA G-quadruplex structures[24-28] that are formed by G-rich sequences interrupted by short loops.[29] Thus, hypothesizing that the generally G-rich ALS-related GDCGG miRNAs adopt intra- or intermolecular G-quadruplex structures *in vitro*, we analysed all synthetic miRNAs used in EMSAs above by native agarose gel electrophoresis. RNA G-quadruplexes are destabilized in the presence of lithium ions[30] and only the ALS-related miR-4741 adopted a secondary structure dissolved by lithium ions (Supplementary Fig. 4A). EMSAs in presence of lithium ions revealed slightly decreased binding of the RGG/RG2 domains of the FXPs to miR-4741 while binding to miR-4745-5p was not affected (Supplementary Fig. 4B). We therefore conclude that G-quadruplex formation of the respective miRNA may enhance but is not required for binding of the FXPs. To exclude that FXP binding of miRNAs is mediated by G-rich sequences alone, we also repeated the Ni-NTA based co-purification approach described above with recombinant full-length FXR1 and a G-rich miRNA without the GDCGG motif. We observed preferential binding of the GDCGG miRNAs compared to the G-rich miRNA without the GDCGG motif (Supplementary Fig. 4C). Hence, all three members of the FXP family directly and predominantly interact with the ALS-related GDCGG miRNAs via their RGG/RG2 domains.

Importantly, endogenous GDCGG motif-containing miRNAs also showed a preferential association with FXR1, as demonstrated by immunoprecipitation of myc-FXR1 and endogenous FXR1 from HEK293 cells followed by qRT-PCR quantification of co-precipitating miRNAs (Fig. 4). This further corroborates FXP/miRNA-interaction *in vivo*. Of note, the GDCGG miRNAs quantified in this assay were previously validated to be downregulated in serum of patients with fALS.[7]

Transcriptome-wide validation of the interaction of fragile X proteins with ALS-related miRNAs

We extended the above findings to a transcriptome-wide level in a fully controlled *in vitro* approach. We incubated each of the recombinant RGG/RG2 domains of FMR1, FXR1 and FXR2 (Fig. 3C and D) with low molecular weight RNA (RNA roughly $\leqslant$ 200 bases) isolated from HEK293 cells followed by recovery using Ni-NTA beads. The co-purifying RNAs were compared to the input RNA using miRNA microarrays interrogating 1733 different mature miRNAs and 1658 miRNA precursors (pre-miRNAs; Affymetrix miRNA 3.0 array). RNAs that were at least 2-fold enriched over the input RNA (corrected *P*-value $\leqslant$ 0.05) were considered as binding to the respective RGG/RG2 domain.

Higher amounts of low molecular weight RNA (~2.5-fold; Fig. 5A) and specifically mature miRNAs (~4.3-fold; Fig. 5B) co-purified with the RGG domain of FXR1 than with the respective domains of FXR2 or FMR1, while the different RGG/RG2 domains were equally recovered (Fig. 5C). A control protein (GST with N-terminal T7 and C-terminal His_6 tags) did not lead to the enrichment of detectable amounts of low molecular weight RNA or mature miRNA (Fig. 5A and B).

The RGG/RG2 domains of the FXPs were associated with approximately one-quarter to one-third of cellular mature miRNAs (Supplementary Table 8), with a large overlap between the different RGG/RG2-domains (Fig. 5D). A hierarchical cluster analysis (average linkage) based on the 101 miRNAs bound by all three RGG/RG2 domains revealed similar specificities of FXR1 and FMR1 in regard to the recovered RNA pattern, while the specificity of the RG2 domain of FXR2 was slightly distinct (Fig. 5E). While all three

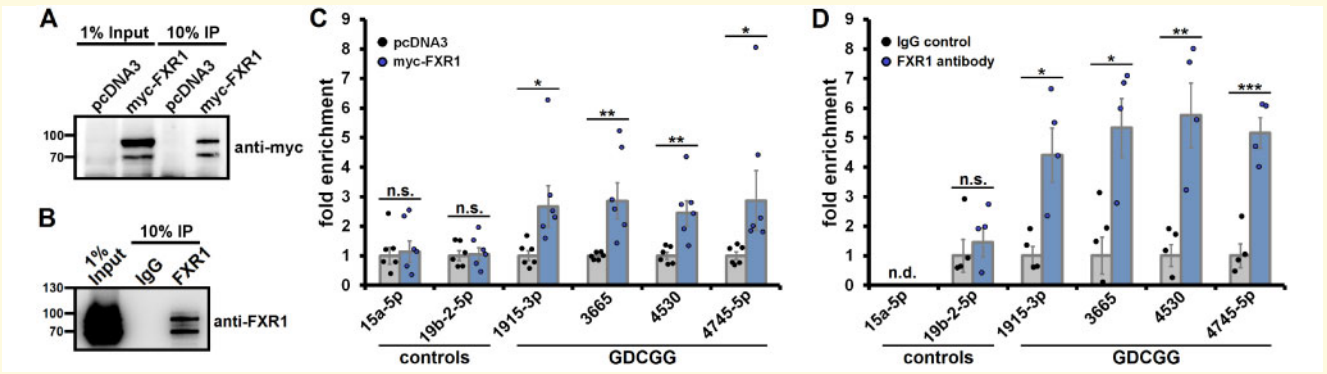

Figure 4 RNA immunoprecipitation of myc-FXR1 and endogenous FXR1 suggests FXP/miRNA interaction *in vivo*. Myc-FXR1 or endogenous FXR1 were immunoprecipitated from lysates of HEK293 cells overexpressing N-terminally myc-tagged FXR1 (isoform a) or from untreated HEK293 lysates, respectively. Co-precipitating miRNAs were quantified by qRT-PCR. (**A** and **B**) Representative western blots showing immunoprecipitations of myc-FXR1 (**A**) and endogenous FXR1 (**B**). (**C** and **D**) Quantitative RT-PCR quantification of mature miRNAs co-precipitating with myc-FXR1 (**C**) and endogenous FXR1 (**D**) (n = 6 or 4, respectively; bars indicate mean ± SEM; $*P \leqslant 0.05$,$**P \leqslant 0.01$, $***P \leqslant 0.001$ in an unpaired, two-tailed Student's *t*-test; n.s. = not significant; n.d. = not detected).

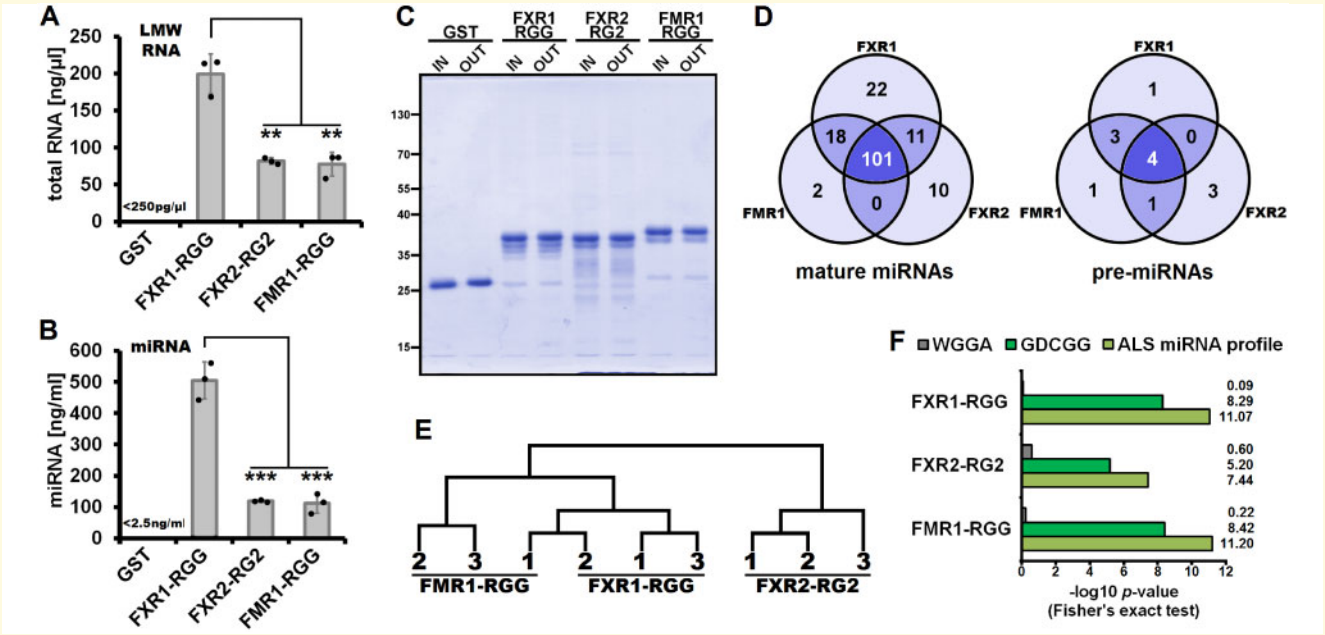

Figure 5 Microarray analyses of miRNAs binding to the RGG/RG2 domains of FXR1, FXR2 and FMR1. (**A** and **B**) Quantification of total RNA (**A**) and miRNA (**B**) co-purifying with the respective RGG/RG2-domains after incubation with low molecular weight (LMW) RNA isolated from HEK293 cells ($n = 3$; bars indicate mean ± SD; $^{**}P \leq 0.01$,$^{***}P \leq 0.001$ in an unpaired, two-tailed Student's *t*-test). (**C**) SDS-PAGE stained with Coomassie brilliant blue comparing the quantity of input protein (IN = 1.5 µg) to the protein recovered using Ni-NTA beads (OUT = 1.5 µl of beads theoretically corresponding to 1.5 µg of protein) in experiments for microarray analyses. (**D**) Venn diagrams visualizing the overlap of mature miRNAs (*left*) or pre-miRNAs (*right*) co-purifying with the RGG/RG2-domains of FXR1, FXR2 and FMR1. (**E**) Hierarchical cluster analysis (average linkage) of the 101 mature miRNAs binding to the RGG/RG2 domains of all three FXP family members. (**F**) Enrichment of miRNAs containing the GDCGG or WGGA motif as well as of the 22 ALS-related miRNAs by the different FXP RGG/RG2 domains. Presence of the respective motif or classification as 'ALS-related' in FXP-binding miRNAs was compared to miRNAs not binding to the different RGG/RG2 domains using Fisher's exact test.

RGG/RG2 domains significantly enriched for GDCGG-containing miRNAs and also for the 22 ALS-related miRNAs, this was less pronounced for the RG2 domain of FXR2. While FXR1 and FMR1 enriched for all 22 or 21 ALS-related miRNAs, respectively, 18 of these miRNAs were bound by FXR2. The mRNA-motif previously supposed to bind most robustly to the RGG-box of FMR1 (WGGA; W = A or U[27,31,32]) was not enriched (Fig. 5F).

In contrast to mature miRNAs, only few pre-miRNAs were enriched by the three different FXP RGG/RG2 domains, indicating a preferential binding to (single stranded) mature miRNAs rather than the hairpin-shaped pre-miRNAs (Fig. 5D and Supplementary Table 9).

FXR1 and FXR2 neuropathology in patients with familial or sporadic ALS

Having shown that FXPs are direct interactors of ALS-associated GDCGG miRNAs, we hypothesized that systemic changes in either expression or cellular distribution of FXPs could be the reason for altered levels of this miRNA subset in serum of ALS patients. FMR1 has indeed been shown to localize to neuronal cytoplasmic inclusions of FUS^{R521C} or TDP-43 in spinal motor neurons of fALS and sALS patients, respectively.[5] We used post-mortem tissue (spinal cord) from fALS (*FUS*- and *C9orf72*-linked) and sALS patients as well as from age-matched control cases to clarify a possible FXR1 and FXR2 pathology. DAB immunohistochemistry of lumbar spinal cord of control patient tissue showed FXR1 and FXR2 co-localized with Nissl bodies and subplasmalemmal cisternae in alpha motor neurons (α-MNs) (Fig. 6A and B). In contrast, α-MNs of both fALS and sALS patients displayed a far more heterogenous FXR1/2 expression level. FXR1 and FXR2 immunoreactivity was either robustly increased [mostly associated with the endoplasmatic reticulum (ER)], or clearly below the level in control sections that had been stained in parallel. In about 30–40% of α-MNs of fALS and sALS patients with elevated immunoreactivity, larger FXR1- and FXR2-positive accumulations were observed (Fig. 6). In α-MNs with decreased immunoreactivity, a more granular, speckled pattern of cytoplasmic FXR2 was found (Fig. 6B).

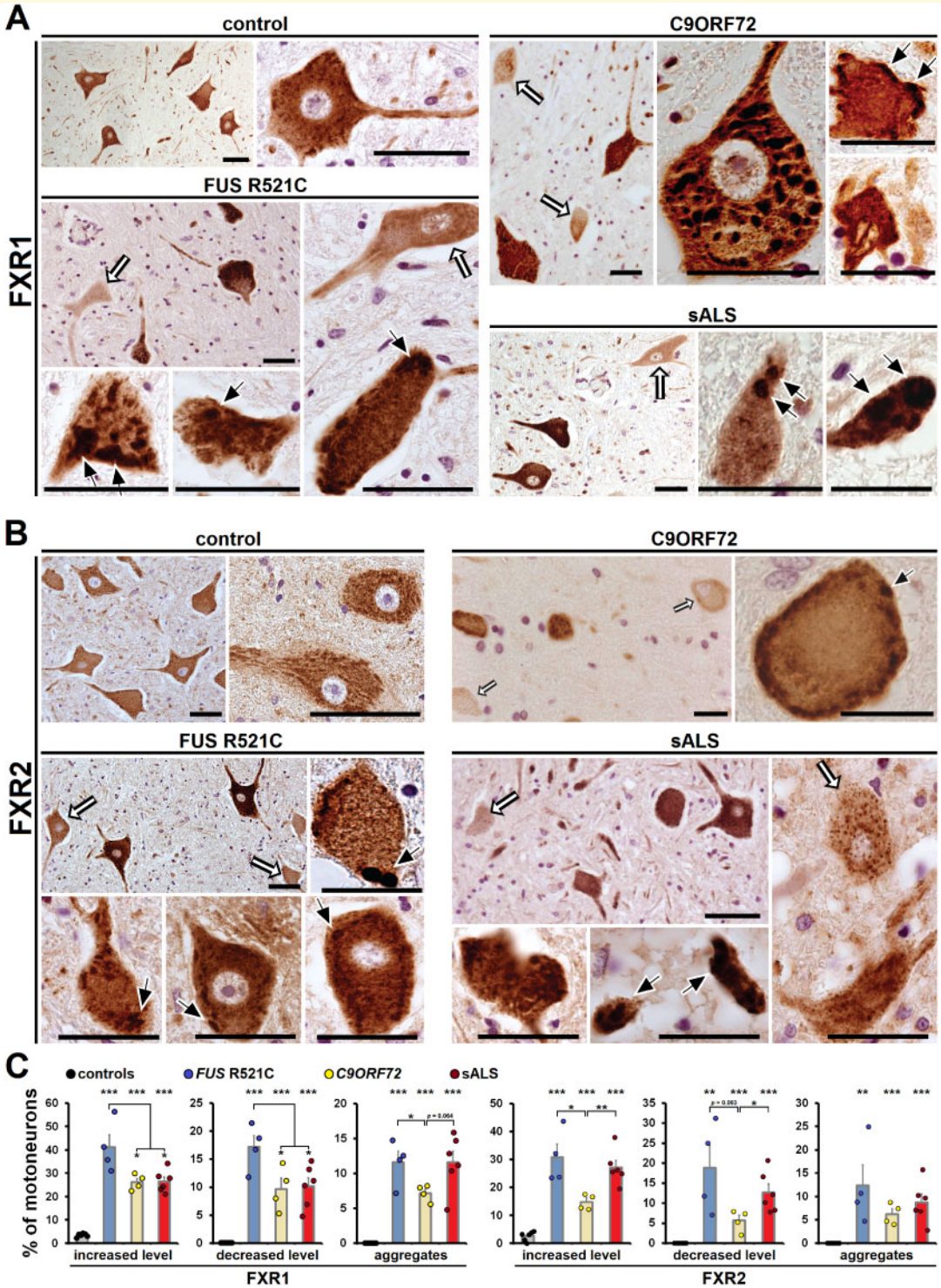

Figure 6 FXR1 and FXR2 are altered in human lumbar spinal cord α-MNs of sALS and fALS patients. (**A**) FXR1and (**B**) FXR2 show moderate, predominantly Nissl substance-associated staining of normal control α-MNs. In sALS as well as in *C9orf72*- and *FUS*-linked fALS, FXR1 and FXR2 immunoreactivity of up to ∼40% of α-MNs is enhanced while labelling of ∼5–20% is reduced (white arrows). Note the more granular, speckled pattern of cytoplasmic FXR2 immunoreactivity that was often seen in sALS and fALS α-MNs with reduced FXR2 staining intensity. Focal, subplasmalemmal larger structures intensely labelled for FXR1 or FXR2, respectively, were prominent in α-MNs of sALS and fALS cases and possibly correspond to enlarged cisternae of the ER and/or accumulations/aggregates of FXR1 and FXR2 (black arrows; scale bars = 60 μm). (**C**) Quantification of aberrant expression (compared to the mean intensity of control staining) and accumulation of FXR1 and FXR2 in spinal cord α-MNs of controls and ALS cases studied [n = 6 controls, 4 FUS^{R521C}, 4 *C9orf72* and 6 sALS; 54 ± 24 (mean ± SD) motor neurons analysed each; bars indicate mean ± SEM; $^{*}P \leqslant 0.05$, $^{**}P \leqslant 0.01$, $^{**}P \leqslant 0.001$ in an unpaired, two-tailed Student's *t*-test; asterisks represent *P*-values compared to the controls].

Fragile X proteins co-aggregate with FUS in iPSC-derived motor neurons

FMR1 has been implicated in ALS pathogenesis and shown to bind to FUS protein before.[5,33] Therefore, we aimed to validate our findings in more detailed analyses and chose FUS-linked ALS as a model of fALS.

In bacterial artificial chromosome (BAC)-transgenic HeLa cells expressing endogenous levels of GFP-tagged FUS^{wt} or ALS-causing FUS^{P525L},[34] all three FXPs clearly localize to spontaneously formed cytoplasmic aggregates of FUS^{P525L}-GFP (Supplementary Fig. 5). Similarly, we found that, in iPSC-derived $FUS^{D502Tfs27}$ motor neurons,[19] FMR1 and FXR1 proteins are detected in spontaneously formed cytoplasmic FUS aggregates. In contrast, co-localization of FXR2 with $FUS^{D502Tfs27}$ was comparatively weak or absent (Supplementary Fig. 6). Therefore, our data indicate co-aggregation of FMR1 and FXR1 with cytoplasmic mutant FUS. The distribution of FXR2 is less clear and its presence in cytoplasmic aggregates may depend on the specific mutation.

More detailed analyses were performed in isogenic iPSC-derived motor neurons expressing endogenously GFP-tagged (using CRISPR/Cas9-editing) FUS^{wt} or pathogenic FUS^{P525L}.[17] Under basal conditions, and further enhanced upon induction of stress granules by sodium arsenite, quantitative co-localization analyses revealed an increased correlation (Pearson's *r*) of the signals of all three FXPs with FUS^{P525L}-GFP when compared to FUS^{wt}-GFP (Fig. 7A–D and Supplementary Fig. 7), indicating co-localization of FXPs specifically with mutant FUS. This is not too surprising, because cytoplasmic mislocalization and formation of stress granule-related FUS granules is a feature of ALS-linked FUS variants. However, considering that there is already convincing evidence for an active contribution of the FXPs to ALS pathogenesis in *in vivo* models,[5,35] these data clearly show alterations of the FXPs in human *FUS* mutant iPSC-derived motor neurons. Moreover, given that iPSC-derived motor neurons most likely represent an early or even pre-symptomatic stage of the disease, these results are in line with presymptomatic downregulation of GDCGG miRNAs.[7] Importantly, three of four tested GDCGG miRNAs previously shown to be downregulated in serum of fALS patients[7] were also less abundant in the FUS^{P525L}-GFP expressing motor neurons (Fig. 7E). In contrast, the majority of the control miRNAs without GDCGG motif used throughout the study were unaffected and argue against a general ALS-related defect in miRNA biogenesis,[36] at least in FUS mutant motor neurons. Fluorescent *in situ* hybridization of FXP-binding miR-3665 or not FXP-binding miR-92a-3p (Fig. 3), confirmed downregulation of miR-3665 in motor neurons expressing mutant FUS. Interestingly, induction of stress granules by sodium arsenite led to reduced abundances of miR-3665 (Fig. 7F and G). Additionally, quantitative co-localization analysis of FXR1 and miRNA signals revealed a higher correlation coefficient (Pearson's *r*) for miR-3665 than for miR-92a-3p, suggesting that the FXP/miRNA interaction characterized above also occurs in human motor neurons (Fig. 7H). However, generally low correlation coefficients may indicate that only a fraction of miR-3665 is associated with FXR1. Interestingly, arsenite treatment decreased the co-localization of miR-3665 with FXR1 in both FUS^{wt}-GFP- and FUS^{P525L}-GFP-expressing motor neurons (Fig. 7H). In contrast, neither the abundance nor the co-localization with FXR1 of miR-92a-3p was altered by the pathogenic FUS mutation or arsenite treatment (Fig. 7G and H).

Recruitment of FXR1 and FXR2 to mutant FUS granules is independent of FMR1

In contrast to FMR1,[5] FXR1 and/or FXR2 did not turn out to be direct interactors of FUS. We performed GST pull-down assays using HEK293 cell lysates and the first 200 amino acids of FMR1 previously shown to mediate the binding to FUS,[33] as well as the respective homologous regions of FXR1 (amino acids 1–200) and FXR2 (amino acids 1–210). These experiments confirmed only the interaction of FMR1 but not FXR1/2 with FUS. The results were independent of the presence of RNA in the lysates (Supplementary Fig. 8).

Moreover, recruitment of FXR1 and FXR2 to mutant FUS aggregates was independent of FMR1, which interacts with both FXR1 and FXR2.[37-39] Here, we used a haploid fibroblast-like *FMR1* knockout cell line. Interestingly, knockout of *FMR1*, and further enhanced by an additional ~50% knockdown of FXR2, led to a dramatic increase of GDCGG miRNAs. In contrast, reduced FXPs had little or no effect on the abundance of control miRNAs further strengthening a possible link of FXPs and ALS-related GDCGG miRNAs (Supplementary Fig. 9). Overexpression of N-terminally myc-tagged FUS^{R495X}, a variant causing early-onset ALS with a fast disease progression[40] led to the spontaneous formation of cytoplasmic FUS aggregates. Almost all these aggregates partially or fully co-localized with FXR1 and FXR2 despite the absence of FMR1 (Supplementary Fig. 10). Similarly, FMR1 was not required for the recruitment of FXR1 and FXR2 to arsenite-induced stress granules (Supplementary Fig. 11). Hence, alternative mechanisms other than (direct) protein-protein interactions with FUS or FMR1 may be responsible for the sequestration of FXR1 and occasionally FXR2 in cytoplasmic aggregates.

FXR1 and FXR2 are differentially altered in FUS-linked ALS

To characterize the co-aggregation of FXR1 and FXR2 with mutant FUS in ALS, we studied post-mortem tissue (lumbar spinal cord) from four fALS patients carrying a FUS^{R521C} mutation as well as age-matched control cases. Similar to

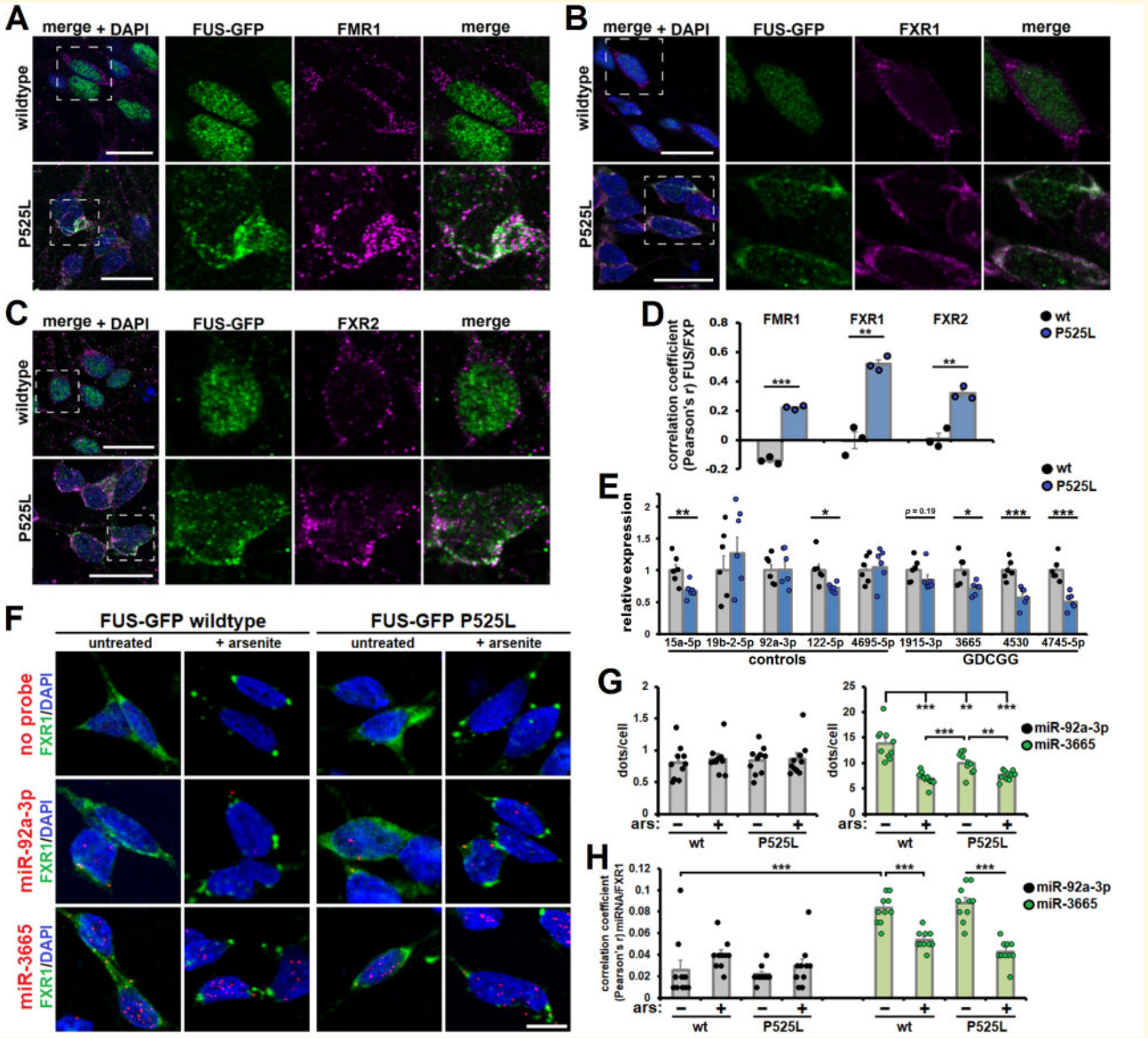

Figure 7 FXPs localize to spontaneous cytoplasmic aggregates of mutant FUS in iPSC-derived motor neurons. (**A**–**C**) Isogenic motor neurons expressing endogenous levels of FUS^{wt}-GFP or FUS^{P525L}-GFP were stained for FMR1 (**A**), FXR1 (**B**) or FXR2 (**C**). White boxes in the overview images on the *left* are shown at higher magnification in the three images on the *right*, respectively (scale bar = 20 μm). (**D**) Co-localization analyses of FUS-GFP and the three FXPs of the staining shown in **A**–**C** ($n = 3$ with 3–14 cells analysed each). (**E**) Relative level of five control miRNAs and four ALS-related GDCGG miRNAs in the isogenic FUS^{wt}-GFP or FUS^{P525L}-GFP motor neurons measured by qRT-PCR. Data were normalized to miR-24-3p and RNU6-2 ($n = 6$). (**F**) Representative images of simultaneous staining of FXR1 and miR-92a-3p or miR-3665, respectively, in isogenic FUS^{wt}-GFP and FUS^{P525L}-GFP motor neurons. Stress granules were induced by addition of 0.2 mM sodium arsenite to the culture medium for 1 h (scale bar = 10 μm). (**G** and **H**) Quantification of dots per cell representing miRNA copies per cell (**G**) and co-localization analyses of FXR1 and miR-92a-3p or miR-3665 (**H**), respectively, of the staining shown in **F** [$n = 2$ with five images analysed each; 62 ± 22 cells/image (mean ± SD); bars indicate mean ± SEM; $^{*}P \leqslant 0.05$, $^{**}P \leqslant 0.01$, ** $P \leqslant 0.001$ in an unpaired, two-tailed Student's *t*-test; 'ars' indicates treatment of cells with 0.2 mM sodium arsenite for 1 h].

the DAB staining earlier (Fig. 6), we detected a pattern of increased ER-associated FXR1 and FXR2 labelling in many, but not all α-MNs. In addition, we found that 18.4% of the FUS aggregates in lumbar spinal cord α-MNs showed a distinct FXR1-immunoreactivity which was usually restricted to the periphery of the inclusions (Fig. 8A and C). Even though few smaller subplasmalemmal aggregates were FXR2 immunoreactive in the DAB-stained sections (Fig. 6B), FUS aggregates and FXR2 immunoreactivity was mutually exclusive in α-MNs of lumbar spinal cords from all FUS mutant cases. Only neurons devoid of FUS inclusions showed FXR2 immunolabelling (Fig. 8B), and FXR2 expression was thus inversely correlated with abnormal FUS accumulation.

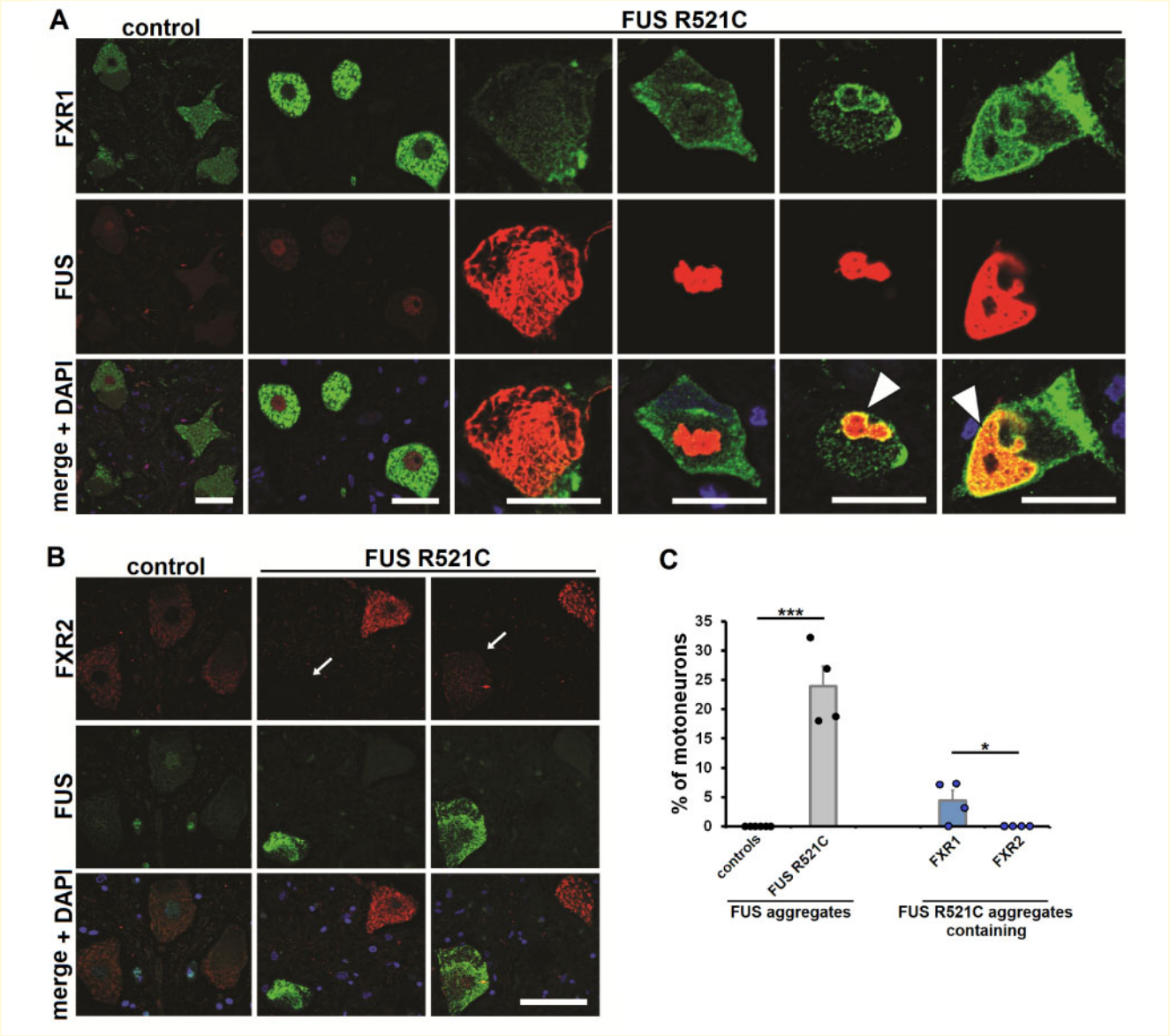

Figure 8 Immunoreactivities of FXR1 and FXR2 correlate with the presence of FUS aggregates in post-mortem tissue of FUS^{R521C} fALS patients. (**A** and **B**) Representative confocal immunofluorescence imaging of human lumbar spinal cord FUS^{R521C} fALS α-MNs. (**A**) Compared to normal controls, FUS^{R521C} α-MNs without FUS aggregates show markedly increased Nissl body-associated FXR1 staining. Cytoplasmic FXR1 immunoreactivity is lower in α-MNs containing FUS aggregates. However, there is strong FXR1-immunoreactivity in the periphery of some (18.4%; white arrowheads), but not all, FUS aggregates. (**B**) Diffuse granular cytoplasmic FXR2 immunoreactivity is present only in those α-MNs that do not show abnormal FUS aggregation. White arrows indicate α-MNs with FUS aggregates and reduced FXR2 staining intensity (scale bar = 60 μm). (**C**) Quantification of FUS aggregates in controls and FUS^{R521C} ALS patients as well as quantification of FXR1 and FXR2 in FUS aggregates of FUS^{R521C} ALS patients [n = 6 controls and 4 FUS^{R521C} ALS patients; 62 ± 25 (mean ± SD) motor neurons analysed each; bars indicate mean ± SEM; *$P \leqslant 0.05$,***$P \leqslant 0.001$ in an unpaired, two-tailed Student's t-test].

Discussion

In our translational work, we managed to draw a bow from peripheral miRNA fingerprints to the discovery of FXP aggregation in CNS neurons. We provide multiple lines of evidence *in vitro*, in cell lines and in human motor neurons that the ALS-linked serum miRNAs directly bind to all three members of the FXP family, FMR1, FXR1 and FXR2, by their shared pentanucleotide consensus sequence. The FXPs were identified based on miRNA alterations detected in both sALS and fALS patients as well as presymptomatic mutation carriers, and we show that FXPs also aggregate in both sALS and fALS motor neurons. This suggests the existence of converging, early pathogenic mechanisms that involve FXPs and are shared between sporadic and familial ALS.

Our data are supported by other unbiased previous screening approaches, e.g. a search for common binding partners of ALS-related proteins[5] or a screen for proteins that are altered by *C9orf72*-associated RNA foci,[41] which suggested that FXPs may be linked to ALS. A comparison of our previous array-based results regarding miRNA expression in ALS patient serum to previous other studies measuring miRNA levels in ALS CNS tissue is difficult, because the ALS-related, generally G-rich miRNAs are poorly covered by small RNA sequencing, or are not included in qRT-PCR-based panels used for miRNA profiling. However, reduced levels of at least some of the ALS-miRNAs binding to the FXPs reported here were found in spinal cord tissue of sALS patients[42] and laser dissected lumbar motor neurons of sALS and fALS patients.[36] In this context, it is also important to note that FXPs, as most proteins linked to ALS pathology, as well as the ALS-related miRNAs are ubiquitously expressed.[43] Therefore, we hypothesize that the ALS-related miRNA profile in serum is rather a reflection of a systemic (including the CNS) downregulation than a direct consequence of affected neurons.

FXPs are known to interact with the miRNA machinery, mainly because of their association with DICER1 and AGO proteins (reviewed in Banerjee *et al.*,[44] and Cheever and Ceman[45]). Further, the presence of pre-miRNAs and mature miRNAs in complexes containing members of the FXP family has been reported *in vivo*.[46] Our findings show that a subset of mature miRNAs directly bind to the RGG/RG2 domains of these proteins without involvement of AGO proteins, which may provide a basis for better understanding not only of FXP functions but also for general miRNA-related gene regulation. Our data add FXPs to the short list of RNA-binding proteins directly interacting with mature miRNAs.[47] Possible FXP functions related to mature miRNAs include but are not limited to shuttling of specific miRNAs to and from AGO proteins, subcellular relocalization of mature miRNAs, miRNA-supported recognition of target mRNAs by FXPs or direct regulation of FXP function by binding of specific miRNAs.

However, the precise connection between FXP function and the observed fingerprint of miRNA alterations in ALS serum remains to be determined. In principle, downregulation of the ALS-related miRNAs (i) may have functional relevance for the pathogenesis of ALS with FXPs being downstream of the miRNA dysregulation; or (ii) alterations of the FXPs may cause the reduced abundance of ALS-related miRNAs in serum, with or without pathogenic relevance of these miRNA alterations. Changes in FXP function or expression placed upstream of ALS-linked miRNA dysregulation may be the more likely possibility, because in HAP1 cells FXP expression was linked to GDCGG miRNA abundance. However, this relation is rather indirect as reduction of FXP level led to an increase of GDCGG miRNA abundance, and other studies argue against an active involvement of FXPs in miRNA biogenesis. For example, FXPs are mostly associated with a mature and active RNA induced silencing complex (RISC) rather than with miRNA biogenesis complexes that contain AGO2 and DICER1.[48] Moreover, a recent screening for RNA-binding proteins involved in the biogenesis of various miRNAs did not identify the FXPs.[49] Additionally, our results show that RGG/RG2 domains of the FXPs are associated with mature miRNAs rather than with miRNA precursors. In contrast, an indirect role of FXPs in miRNA biogenesis is more plausible as FMR1 was previously found to regulate the protein levels of e.g. DROSHA, a ribonuclease catalysing the first processing step of primary miRNA transcripts.[50] Moreover, systemically altered FXP function or expression may in turn cause a differential transport or stability of miRNAs in the serum. Generally, elucidating the physiological function of the association of mature miRNAs with FXPs reported here could lead to valuable insights in the pathogenesis of ALS.

Along the line of previously published data showing that greatly reduced miRNA levels due to genetic ablation of *Dicer1* in mouse motor neurons cause an ALS-like phenotype,[51] it is tempting to speculate that downregulation of the GDCGG miRNAs in ALS may indeed represent a contributor to protein aggregation and ALS pathogenesis. Clearly, further studies are required to verify such a possible scenario. Strongly suggesting a functional role of the systemically altered ALS-linked miRNAs and/or FXPs in ALS pathogenesis is the fact that immunohistochemistry revealed an aberrant expression and aggregation of both FXR1 and FXR2 in fALS and sALS patient spinal cord tissue. Moreover, similar pathological findings are observed for FXR1 and FXR2 in autopsy tissue from ALS linked to *FUS* mutations and consequent FUS protein aggregation, as well as in other ALS cases accompanied by TDP-43 pathology (*C9orf72*-linked and sALS).[1] Together with previous reports showing that FMR1 is a component of both pathological TDP-43 and FUS inclusions,[5] FXPs might turn out to be useful neuropathological markers for ALS with a broader prevalence than observed for phosphorylated TDP-43.

The cellular models used in our work suggest aggregation of all three FXPs in FUS mutant neurons. Considering that human iPSC-derived motor neurons *in vitro* have been suggested to be more representative of early or even presymptomatic stages of neurodegeneration,[52] our results further support that dysregulation of the FXPs is an early event in ALS pathogenesis. While FMR1 and FXR1 seem to be general components of mutant FUS aggregates, co-aggregation of FXR2 may depend on the specific FUS mutation. We show that the co-aggregation of FXR1/2 and FUS does neither depend on (direct) protein-protein interaction between FXR1/2 and FUS, nor on the presence of FMR1, which is an established binding partner of both FXR1/2 and FUS and thus a possible adaptor protein.[5,33,37–39] Therefore, additional factors such as specific proteins or RNAs that remain to be determined might attract FXR1 and occasionally FXR2 to aggregated FUS.

Neuropathological studies revealed accumulation of FXR1 at the margins of some, but not all, FUS^{R521C} inclusions in α-MNs, raising the hypothesis that FXR1 may play a role in

the clearance or shielding of pathological aggregates. Surprisingly, in post-mortem spinal cord α-MNs, FXR2 expression, and to a lesser extend the expression of FXR1, were inversely correlated with the presence of FUS inclusions. Moreover, FXR2 immunoreactivity and FUS inclusions were mutually exclusive, i.e. only motor neurons virtually lacking FXR2 expression contained FUS aggregates.

Taken together, our data indicate a role of the FXPs in pathogenic protein aggregation, at least in sporadic, *C9orf72*- and *FUS*-linked ALS. The fact that a molecular pattern in blood ultimately led to the identification of novel neuropathological markers of ALS strengthens the view of ALS as a systemic disease. Our unconventional and unbiased experimental strategy strongly suggests that systemic molecular pathology can reflect neurodegeneration-related alterations in the CNS and help to find novel disease-related molecules. Notably, the ALS-related serum miRNA profiles that led to the identification of FXPs in our translational approach were already evident in preclinical carriers of causative ALS mutations.[7] Therefore, our results presented here could be the first step in uncovering a novel pathogenic pathway altered many years before actual onset of symptomatic disease in the majority of ALS patients.

Acknowledgements

We acknowledge the Netherlands ALS foundation and thank the team that contributed to the establishment of the Dutch ALS Tissue Bank (Prof. Dr D. Troost and Prof. Dr M. de Visser). We thank Jasper Anink, Caroline Mijnsbergen (AMC, Amsterdam) and Jette Abel (University of Rostock) for excellent technical support and Prof. S. Gründer (Institute of Physiology, RWTH Aachen University Hospital) for generous support in confocal laser scanning microscopy. We also thank Anthony A. Hyman (Max Planck Institute of Molecular Cell Biology and Genetics, Dresden, Germany) for providing BAC-transgenic HeLa cells.

Funding

This work was supported by the German Motor Neuron Disease Network (BMBF-MND-Net; Funds 360644) (J.W.), the EU Joint Program Neurodegenerative Diseases (JPND) (J.W., J.H.W.), the Interdisciplinary Centre for Clinical Research (IZKF Aachen, N7-4) (J.W., A.G.), the NOMIS foundation (A.H.), the Helmholtz Virtual Institute "RNA dysmetabolism in ALS and FTD (VH-VI-510)" (A.H.), the Swedish Brain Foundation (2012-0262, 2012-0305, 2013-0279, 2016-0303, 2020-0353) (P.M.A.), the Swedish Science Council (2012-3167, 2017-03100) (P.M.A.), the Knut and Alice Wallenberg Foundation (2012.0091, 2014.0305, 2020.0232) (P.M.A.), the Ulla-Carin Lindquist Foundation (P.M.A.), the King Gustaf V:s and Queen Victoria's Freemason's Foundation, the German Society for patients with Neuromuscular Diseases (DGM) (A.G., J.W., J.H.W.), the Initiative Therapieforschung ALS e. V. (A.G., J.W.) and the Stichting ALS Nederland (E.A.). A.H. is supported by the Hermann und Lilly Schilling-Stiftung für medizinische Forschung im Stifterverband.

Competing interests

The authors report no competing interests.

Supplementary material

Supplementary material is available at *Brain* online.

References

1. Al-Chalabi A, Jones A, Troakes C, King A, Al-Sarraj S, van den Berg LH. The genetics and neuropathology of amyotrophic lateral sclerosis. *Acta Neuropathol*. 2012;124:339-352.
2. Brown RH, Al-Chalabi A. Amyotrophic lateral sclerosis. *N Engl J Med*. 2017;377:162-172.
3. Hardiman O, Al-Chalabi A, Chio A, et al. Amyotrophic lateral sclerosis. *Nat Rev Dis Primers*. 2017;3:17071.
4. Weishaupt JH, Hyman T, Dikic I. Common molecular pathways in amyotrophic lateral sclerosis and frontotemporal dementia. *Trends Mol Med*. 2016;22:769-783.
5. Blokhuis AM, Koppers M, Groen EJ, et al. Comparative interactomics analysis of different ALS-associated proteins identifies converging molecular pathways. *Acta Neuropathol*. 2016;132:175-196.
6. Mao Y, Kuo SW, Chen L, Heckman CJ, Jiang MC. The essential and downstream common proteins of amyotrophic lateral sclerosis: A protein-protein interaction network analysis. *PLoS One*. 2017;12:e0172246.
7. Freischmidt A, Muller K, Zondler L, et al. Serum microRNAs in patients with genetic amyotrophic lateral sclerosis and pre-manifest mutation carriers. *Brain*. 2014;137:2938-2950.
8. Freischmidt A, Muller K, Zondler L, et al. Serum microRNAs in sporadic amyotrophic lateral sclerosis. *Neurobiol Aging*. 2015;36:2660.e15-20.
9. Turchinovich A, Weiz L, Burwinkel B. Extracellular miRNAs: The mystery of their origin and function. *Trends Biochem Sci*. 2012;37:460-465.
10. Brooks BR, Miller RG, Swash M, Munsat TL; World Federation of Neurology Research Group on Motor Neuron Diseases. El Escorial revisited: Revised criteria for the diagnosis of amyotrophic lateral sclerosis. *Amyotroph Lateral Scler Other Motor Neuron Disord*. 2000;1:293-299.
11. Zondler L, Muller K, Khalaji S, et al. Peripheral monocytes are functionally altered and invade the CNS in ALS patients. *Acta Neuropathol*. 2016;132:391-411.
12. Huang da W, Sherman BT, Lempicki RA. Bioinformatics enrichment tools: Paths toward the comprehensive functional analysis of large gene lists. *Nucleic Acids Res*. 2009;37:1-13.
13. Huang da W, Sherman BT, Lempicki RA. Systematic and integrative analysis of large gene lists using DAVID bioinformatics resources. *Nat Protoc*. 2009;4:44-57.
14. Walia RR, Xue LC, Wilkins K, El-Manzalawy Y, Dobbs D, Honavar V. RNABindRPlus: A predictor that combines machine learning and sequence homology-based methods to improve the

reliability of predicted RNA-binding residues in proteins. *PLoS One*. 2014;9:e97725.
15. Liu W, Xie Y, Ma J, et al. IBS: An illustrator for the presentation and visualization of biological sequences. *Bioinformatics*. 2015;31: 3359-3361.
16. Sturn A, Quackenbush J, Trajanoski Z. Genesis: Cluster analysis of microarray data. *Bioinformatics*. 2002;18:207-208.
17. Naumann M, Pal A, Goswami A, et al. Impaired DNA damage response signaling by FUS-NLS mutations leads to neurodegeneration and FUS aggregate formation. *Nat Commun*. 2018;9:335.
18. Chitiprolu M, Jagow C, Tremblay V, et al. A complex of C9ORF72 and p62 uses arginine methylation to eliminate stress granules by autophagy. *Nat Commun*. 2018;9:2794.
19. Higelin J, Demestre M, Putz S, et al. FUS mislocalization and vulnerability to DNA damage in ALS patients derived hiPSCs and aging motoneurons. *Front Cell Neurosci*. 2016;10:290.
20. Japtok J, Lojewski X, Naumann M, et al. Stepwise acquirement of hallmark neuropathology in FUS-ALS iPSC models depends on mutation type and neuronal aging. *Neurobiol Dis*. 2015;82: 420-429.
21. Benjamini Y, Hochberg Y. Controlling the false discovery rate—A practical and powerful approach to multiple testing. *J R Stat Soc B*. 1995;57:289-300.
22. Tsui NB, Ng EK, Lo YM. Stability of endogenous and added RNA in blood specimens, serum, and plasma. *Clin Chem*. 2002; 48:1647-1653.
23. Chromy BA, Gonzales AD, Perkins J, et al. Proteomic analysis of human serum by two-dimensional differential gel electrophoresis after depletion of high-abundant proteins. *J Proteome Res*. 2004;3: 1120-1127.
24. Blice-Baum AC, Mihailescu MR. Biophysical characterization of G-quadruplex forming FMR1 mRNA and of its interactions with different fragile X mental retardation protein isoforms. *RNA*. 2014;20:103-114.
25. Darnell JC, Fraser CE, Mostovetsky O, Darnell RB. Discrimination of common and unique RNA-binding activities among Fragile X mental retardation protein paralogs. *Hum Mol Genet*. 2009;18:3164-3177.
26. Phan AT, Kuryavyi V, Darnell JC, et al. Structure-function studies of FMRP RGG peptide recognition of an RNA duplex-quadruplex junction. *Nat Struct Mol Biol*. 2011;18:796-804.
27. Suhl JA, Chopra P, Anderson BR, Bassell GJ, Warren ST. Analysis of FMRP mRNA target datasets reveals highly associated mRNAs mediated by G-quadruplex structures formed via clustered WGGA sequences. *Hum Mol Genet*. 2014;23:5479-5491.
28. Vasilyev N, Polonskaia A, Darnell JC, Darnell RB, Patel DJ, Serganov A. Crystal structure reveals specific recognition of a G-quadruplex RNA by a beta-turn in the RGG motif of FMRP. *Proc Natl Acad Sci USA*. 2015;112:E5391-E5400.
29. Fay MM, Lyons SM, Ivanov P. RNA G-quadruplexes in biology: Principles and molecular mechanisms. *J Mol Biol*. 2017;429: 2127-2147.
30. Lane AN, Chaires JB, Gray RD, Trent JO. Stability and kinetics of G-quadruplex structures. *Nucleic Acids Res*. 2008;36:5482-5515.
31. Anderson BR, Chopra P, Suhl JA, Warren ST, Bassell GJ. Identification of consensus binding sites clarifies FMRP binding determinants. *Nucleic Acids Res*. 2016;44:6649-6659.
32. Ascano M Jr., Mukherjee N, Bandaru P, et al. FMRP targets distinct mRNA sequence elements to regulate protein expression. *Nature*. 2012;492:382-386.
33. He Q, Ge W. The tandem Agenet domain of fragile X mental retardation protein interacts with FUS. *Sci Rep*. 2017;7:962.
34. Patel A, Lee HO, Jawerth L, et al. A liquid-to-solid phase transition of the ALS Protein FUS accelerated by disease mutation. *Cell*. 2015;162:1066-1077.
35. Coyne AN, Yamada SB, Siddegowda BB, et al. Fragile X protein mitigates TDP-43 toxicity by remodeling RNA granules and restoring translation. *Hum Mol Genet*. 2015;24:6886-6898.
36. Emde A, Eitan C, Liou LL, et al. Dysregulated miRNA biogenesis downstream of cellular stress and ALS-causing mutations: A new mechanism for ALS. *EMBO J*. 2015;34:2633-2651.
37. Huttlin EL, Bruckner RJ, Paulo JA, et al. Architecture of the human interactome defines protein communities and disease networks. *Nature*. 2017;545:505-509.
38. Huttlin EL, Ting L, Bruckner RJ, et al. The BioPlex Network: A systematic exploration of the human interactome. *Cell*. 2015;162: 425-440.
39. Zhang Y, O'Connor JP, Siomi MC, et al. The fragile X mental retardation syndrome protein interacts with novel homologs FXR1 and FXR2. *EMBO J*. 1995;14:5358-5366.
40. Bosco DA, Lemay N, Ko HK, et al. Mutant FUS proteins that cause amyotrophic lateral sclerosis incorporate into stress granules. *Hum Mol Genet*. 2010;19:4160-4175.
41. Rossi S, Serrano A, Gerbino V, et al. Nuclear accumulation of mRNAs underlies G4C2-repeat-induced translational repression in a cellular model of C9orf72 ALS. *J Cell Sci*. 2015;128:1787-1799.
42. Figueroa-Romero C, Hur J, Lunn JS, et al. Expression of microRNAs in human post-mortem amyotrophic lateral sclerosis spinal cords provides insight into disease mechanisms. *Mol Cell Neurosci*. 2016;71:34-45.
43. Ludwig N, Leidinger P, Becker K, et al. Distribution of miRNA expression across human tissues. *Nucleic Acids Res*. 2016;44: 3865-3877.
44. Banerjee A, Ifrim MF, Valdez AN, Raj N, Bassell GJ. Aberrant RNA translation in fragile X syndrome: From FMRP mechanisms to emerging therapeutic strategies. *Brain Res*. 2018;1693:24-36.
45. Cheever A, Ceman S. Translation regulation of mRNAs by the fragile X family of proteins through the microRNA pathway. *RNA Biol*. 2009;6:175-178.
46. Jin P, Zarnescu DC, Ceman S, et al. Biochemical and genetic interaction between the fragile X mental retardation protein and the microRNA pathway. *Nat Neurosci*. 2004;7:113-117.
47. Zealy RW, Wrenn SP, Davila S, Min KW, Yoon JH. microRNA-binding proteins: Specificity and function. *Wiley Interdiscip Rev RNA*. 2017;8:e1414.
48. Schopp IM, Amaya Ramirez CC, Debeljak J, et al. Split-BioID a conditional proteomics approach to monitor the composition of spatiotemporally defined protein complexes. *Nat Commun*. 2017; 8:15690.
49. Treiber T, Treiber N, Plessmann U, et al. A compendium of RNA-binding proteins that regulate microRNA biogenesis. *Mol Cell*. 2017;66:270-284.e13.
50. Wan RP, Zhou LT, Yang HX, et al. Involvement of FMRP in primary MicroRNA processing via enhancing Drosha translation. *Mol Neurobiol*. 2017;54:2585-2594.
51. Haramati S, Chapnik E, Sztainberg Y, et al. miRNA malfunction causes spinal motor neuron disease. *Proc Natl Acad Sci USA*. 2010;107:13111-13116.
52. Guo W, Fumagalli L, Prior R, Van Den Bosch L. Current advances and limitations in modeling ALS/FTD in a dish using induced pluripotent stem cells. *Front Neurosci*. 2017;11:671.